Preparation and Evaluation of Solid Dispersion for Nitrendipine–Carbopol and Nitrendipine–HPMCP Systems Using a Twin Screw Extruder

Liang WANG,[a] Fu De CUI,[a] Tomokazu HAYASE,[b] and Hisakazu SUNADA*,[b]

[a] *Department of Pharmaceutics, Shenyang Pharmaceutical University; No. 103, Wenhua Road, Shenyang 110016, P.R. China: and* [b] *Faculty of Pharmacy, Meijo University; 150 Yagotoyama, Tempaku-ku, Nagoya 468–8503, Japan.*
Received April 25, 2005; accepted July 20, 2005

In the present study, we prepared solid dispersions of the poorly water-soluble drug nitrendipine (NIT) using the twin screw extruder method with high-molecular-weight substances, hydroxypropylmethylcellulosephthalate (HPMCP) and Carbopol (CAR), as carriers. Powder X-ray diffraction (PXRD) and differential scanning calorimetry (DSC) evaluation showed that solid dispersions can be formed when NIT–HPMCP and NIT–CAR mixtures are treated with the twin screw extruder method. Fourier Transformation IR Spectroscopy (FT-IR) obtained with NIT–HPMCP and NIT–CAR solid dispersions indicated the presence of hydrogen bonding between the drug and the carriers. NIT–CAR solid dispersions were found to give somewhat higher dissolution than crystalline NIT and physical mixtures, while the dissolution of NIT–HPMCP solid dispersions was markedly decreased compared with the crystalline NIT and physical mixtures. These findings indicated that CAR has a greater ability to improve the dissolution of NIT than HPMCP when a twin screw extruder was employed to prepare the solid dispersions. The twin screw extruder method can be used as a simple and effective method for the preparation of solid dispersions to improve the dissolution properties of poorly water-soluble drugs when choosing proper polymers as carriers.

Key words solid dispersion; twin screw extruder; nitrendipine; Carbopol; hydroxypropylmethylcellulosephthalate (HPMCP)

The use of poorly water-soluble drugs has a number of drawbacks, such as increasing the dosage, the administration frequency and the resultant occurrence of side effects. Furthermore, as the rate-limiting step in the absorption process for poorly water-soluble drugs is the dissolution rate of such drugs in the gastrointestinal fluids rather than the rapidity of their diffusion across the gut wall, it is important to improve the oral bioavailability of poorly water-soluble drugs by improving their dissolution rate and solubility. This remains one of the most challenging aspects of drug development.

The solid dispersion (SD) method, by which a drug is dispersed in a carrier to make it amorphous, is one of the pharmaceutical approaches most commonly employed to enhance bioavailability of poorly water-soluble drugs.[1—3)]

Various pharmaceutical approaches for the preparation of SDs, including coprecipitation, lyophilization, spray drying, solvent evaporation, fusion and powder mixing methods, have been reported.[4)] An important mechanism is the reduction of the drug's particle size to the microcrystalline or molecular level for rapid dissolution and absorption. Broadly speaking, there are three methods of preparing SDs; namely, the fusion method, the solvent process and a combination of these.[2)] However, the fusion method and solvent method have a number of drawbacks.[5,6)] The fusion method requires a high temperature which may result in the decomposition of the drugs, and furthermore, tacky or glassy solids may cause undesirable processing problems.[7)] In the solvent method, environmental concerns regarding solvent emissions and heath concerns regarding residual solvent make it necessary to restrict the use of organic solvent.[5)]

A heating/pressurization/kneading/extruding method using a twin screw extruder is one of the methods proposed for this purpose.[8)] This extruder, originally designed as an extraction/casting device for polymer alloys in the plastic industry,[9)] is now used to process cereals and "functionalize" food materials, such as tissue products from animal protein.[10)] This device has already been used successfully to prepare SDs of nifedipine and hydroxypropylmethylcellulosephthalate (HPMCP),[11)] itraconazole and hydroxypropylmethylcellulose (HPMC),[12,13)] itraconazole and hydroxypropyl-beta-cyclodextrin (HP-beta-CD)[13)] to improve the solubility and dissolution properties of poorly water-soluble drugs. Six *et al.*[14)] prepared SDs of itraconazole-Eudragit E100/PVPVA64 and found that the combination of the two polymers provides an SD with good dissolution properties and improved physical stability compared with the binary SDs of itraconazole. Kinoshita *et al.*[15)] prepared SDs of TAS-301, a poorly water-soluble drug, and a porous calcium silicate (FLR) using the twin screw extruder method. The solubility and bioavailability of TAS-301 were markedly enhanced by its melt-adsorption on FLR.

These findings suggest that the twin screw extruder method is a useful technique for preparing SDs and improving the solubility and bioavailability of poorly water-soluble drugs. One of its advantages is that there is no need for the use of organic solvents during the process of preparation. Moreover, SDs can be produced at a lower temperature than the melting point of the drug and the softening temperature of the polymer, preventing the decomposition of the drug and carriers. In addition, various combinations of carriers can be employed to prepare SDs with improved dissolution and physical stability properties than the binary SDs.[14)]

Nitrendipine (NIT) is a dihydropyridine calcium channel blocking agent[16)] producing peripheral vasodilation as its predominant *in vivo* effect. The molecular structure of NIT is illustrated in Fig. 1. NIT shares a common dihydropyridine nucleus with the calcium antagonist, nifedipine. Like nifedipine, NIT is used to treat a variety of cardiovascular disorders, such as angina pectoris and hypertension.[17)] NIT exists in the form of yellow crystals with a melting point of 156—159 °C. Due to its low aqueous solubility (about 2 μg/ml), leading to the poor absorption of NIT after oral administration, NIT

* To whom correspondence should be addressed. e-mail: sunada@ccmfs.meijo-u.ac.jp

Table 1. Properties of Carbopol 971-P-NF(CAR) and Its Gel Structure

Polymer (grade)	Density (g/cm^3)	MW[a)]	Viscosity[b)] (CPS)	Polymerization solvent	Gel structure
CAR 971-P-NF	1.41	1250000	4000—11000	Ethyl acetate	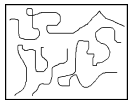 Fishnet

a) Nominal-average molecular weight. *b*) 0.5% solution, 25 °C, pH 7.5.

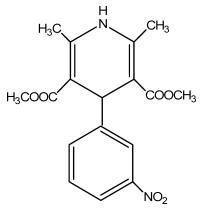

Fig. 1. Molecular Structure of Nitrendipine

often shows low and irregular bioavailability following oral administration.[18)]

In the present study, SDs of NIT with HPMCP and Carbopol® 971-P-NF (CAR), a cross-linked polymer of acrylic acid with the fishnet gel structure shown in Table 1, as carriers were prepared using the twin screw extruder method. The dissolution properties and physicochemical properties of the SDs were investigated and compared with their physical mixtures (PMs).

Experimental

Materials Nitrendipine (NIT) was obtained from Nanjing Pharmaceutical Factory (China); Carbopol 971-P-NF (CAR) from LABOLATORIO CHIMIKO INTERNAZIONALE Co., Ltd., HPMCP (HP-55) from Shin-Etsu Chemical Co., Ltd., Japan and sodium dodecyl sulfate (SDS) from Wako Pure Chemical Industries Co., Ltd., Japan. All other chemicals were of reagent grade. All experiments were carried out under subdued light to prevent the light induced degradation of NIT.

Twin Screw Extruder Method The required amount of NIT and HPMCP or CAR were weighed and mixed by hand in a polyethylene bag for 10 min to obtain PMs. Table 2 summarizes the quantity of each ingredient used in each PM.

The twin screw extruder (KEX-25, Kurimoto, Ltd.) used in the present study consisted of a hopper, barrels, a die, a kneading screw, and heaters. The thread interval of the feed screw decreases from the hopper side to the die side. A PM introduced into the hopper is carried forward by the feed screw, kneaded under high pressure by the kneading screw, and extruded from the die. The temperature inside the barrels can be accurately controlled from 30 to 300 °C with 4 independent heaters, and water can be introduced from the liquid injection port if necessary.

The operating conditions are shown in Table 3. The PMs of NIT–HPMCP were treated with the twin screw extruder at a screw rotation rate of 100 rpm, a powder supply rate of 15 g/min, a water supply rate of 2 ml/min, and a barrel temperature of 105 °C. The PMs of NIT–CAR were treated at a screw rotation rate of 100 rpm, a powder supply rate of 15 g/min, a water supply rate of 0.5 ml/min, and a barrel temperature of 85 °C. Treated mixtures were dried for 10 h using a dryer (inside temperature, 50 °C), pulverized using a QUADRO COMIL (QC-197S, Powlex Co., Ltd.) equipped with a grater-type screen (2.39 mm ϕ), pulverized again using an automatic mortar (Model ANM200 E, Nitto Kagaku Co., Ltd.), and sieved through a 63—250 μm sieve to obtain a sample for granule dissolution. Samples 63 μm or finer were used for powder X-ray diffraction and differential scanning calorimetric analysis.

Evaluation of Solid Dispersions. Powder X-Ray Diffraction (PXRD) Powder X-ray diffraction analysis was performed with a linear X-ray diffraction system (RAD-2VC, Rigaku Denki Co., Ltd.) in which Cu$K\alpha$ rays (40 kV, 20 mA) were used as X-rays. The degree of diffraction was measured at 5°/min every 0.01° between 5 and 45° (2θ).

Table 2. Formulation of Physical Mixtures

Nitrendipine (g)	150	75	50	150	75	50
Carbopol (g)	150	225	250	—	—	—
HPMCP (g)	—	—	—	150	225	250
Total amount (g)	300	300	300	300	300	300

Table 3. Operating Conditions of Twin Screw Extruder

	Barrel temperature (°C)	Powder feed speed (g/min)	Screw revolution speed (rpm)	Water content (ml/min)
NIT–HPMCP	105	15	100	2
NIT–CAR	85	15	100	0.5

Differential Scanning Calorimetry (DSC) DSC analysis was carried out on a differential scanning calorimeter (DSC 60, Shimadzu). All samples were prepared by placing 10 mg of the powder into an aluminum pan for analysis. The thermograms were obtained by heating the samples at a rate of 10 °C/min from 30 °C to 200 °C in atmospheric air. Plots of heat flow *versus* temperature were recorded.

Fourier Transformation-IR Spectroscopy (FT-IR) Drug-carrier interactions in samples were determined based on IR spectra measured with a FT-IR spectroscope (PerkinElmer Spectrum One) by the KBr method in the 4000—450 cm^{-1} region at 4 cm^{-1} resolution at 16 scans per spectrum.

Dissolution Test The amount of drug released from the samples was determined using a dissolution test apparatus (NTR-3000, Toyama Sangyo Co., Ltd.) according to the dissolution test method 2 (paddle method) described in the Japanese Pharmacopoeia (JP) XIII. The paddles were rotated at 100 rpm. Samples equivalent to 20 mg NIT were added to the dissolution medium (900 ml of 0.5% w/v SDS water solution adjusted to 37±0.1 °C). Test fluids (about 5 ml) were withdrawn at predetermined time intervals from each vessel through a glass filter, filtered through a 0.2 μm membrane filter (DISMIC-13CP, Toyo Filter Paper Co., Ltd.) and analyzed for NIT spectrophotometrically at 349 nm with a spectrophotometer (UV-160, Shimadzu Corp.). The same volume of fresh medium was replaced and correction for the cumulative dilution was calculated. The percentage of NIT dissolved for each formula was plotted *versus* time. To obtain the apparent dissolution rate constant, $\ln(M/M_0)$ was calculated using Eq. 1 and plotted *versus* time.

$$\ln(M/M_0) = -K_p t \quad (1)$$

M_0 is the amount of the drug in samples (mg); M is the amount of undissolved drug (mg); K_p is the apparent dissolution rate constant (min^{-1}); t is the time (min).

Results and Discussion

Evaluation of Solid Dispersion. Changes in Crystallinity Powder X-ray diffraction patterns of NIT, HPMCP, their PMs, and NIT–HPMCP treated with the twin screw extruder method are shown in Fig. 2. Pure NIT drug powder showed numerous distinctive peaks (Fig. 2 A) that indicated a

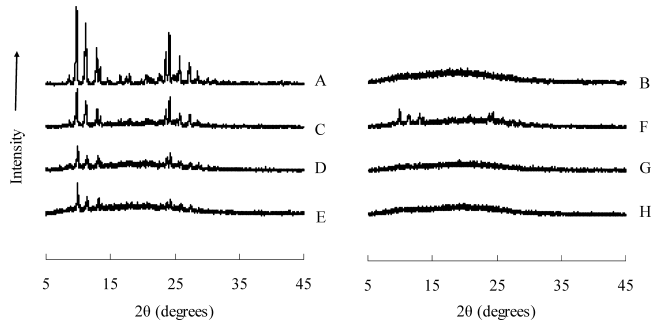

Fig. 2. Powder X-Ray Diffraction Patterns of NIT, HPMCP, PMs and SDs Prepared with the Twin Screw Extruder Method

A, NIT; B, HPMCP; PM, NIT : HPMCP, C, 1 : 1; D, 1 : 3; E, 1 : 5; Twin screw extruder method, NIT : HPMCP, F, 1 : 1; G, 1 : 3; H, 1 : 5.

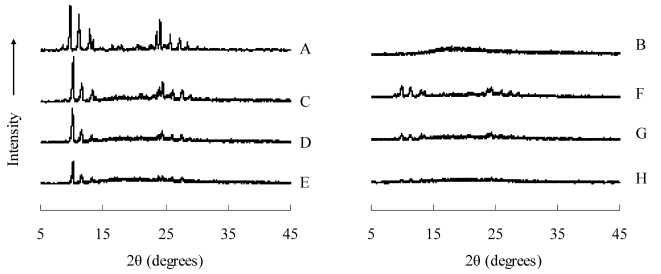

Fig. 3. Powder X-Ray Diffraction Patterns of NIT, CAR, PMs and SDs Prepared with the Twin Screw Extruder Method

A, NIT; B, CAR; PMs, NIT : CAR, C, 1 : 1; D, 1 : 3; E, 1 : 5; Twin screw extruder method, NIT : CAR, F, 1 : 1; G, 1 : 3; H, 1 : 5.

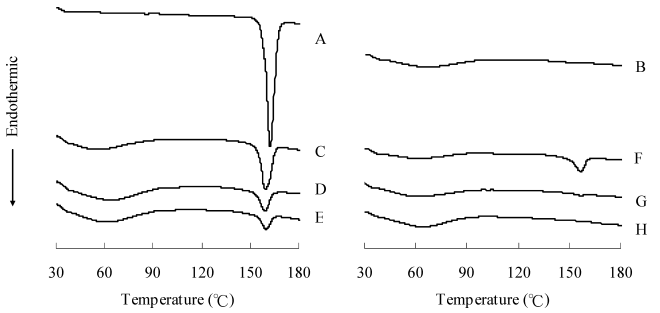

Fig. 4. Differential Scanning Calorimetry Curves of NIT, HPMCP, PMs and SDs Prepared with the Twin Screw Extruder Method

A, NIT; B, HPMCP; PMs, NIT : HPMCP, C, 1 : 1; D, 1 : 3; E, 1 : 5; Twin screw extruder method, NIT : HPMCP, F, 1 : 1; G, 1 : 3; H, 1 : 5.

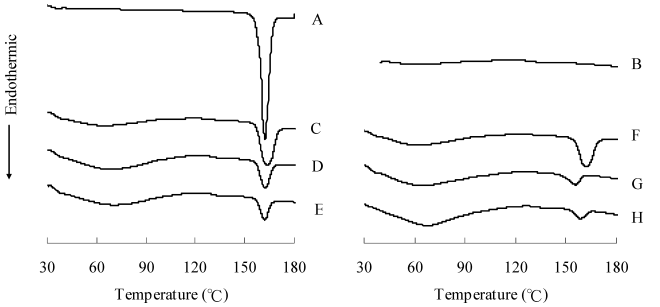

Fig. 5. Differential Scanning Calorimetry Curves of NIT, CAR, PMs and SDs Prepared with the Twin Screw Extruder Method

A, NIT; B, CAR; PMs, NIT : CAR, C, 1 : 1; D, 1 : 3; E, 1 : 5; Twin screw extruder method, NIT : CAR, F, 1 : 1; G, 1 : 3; H, 1 : 5.

high crystallinity. The high-molecular weight carrier HPMCP exhibited a broad diffraction pattern (Fig. 2 B). The PMs showed all the characteristic diffraction peaks of crystalline NIT, but of lower intensity, and furthermore, the peak intensity decreased as the ratio of HPMCP increased. NIT–HPMCP mixtures treated with the twin screw extruder method of 1 : 1 weight ratio of NIT : HPMCP (Fig. 2 F) exhibited a low peak intensity. At a ratio of 1 : 3 and 1 : 5 (Fig. 2 G, H) the distinctive diffraction peaks of NIT disappeared completely, showing a completely hollow pattern of the SD.

Powder X-ray diffraction patterns of the NIT–CAR system are shown in Fig. 3. The carrier CAR exhibited a hollow diffraction pattern (Fig. 3 B). In the PMs, diffraction peaks derived from NIT were observed and attenuated with an increase in the ratio of CAR. On SDs at a ratio of 1 : 1 and 1 : 3 (Fig. 3 F, G), the distinctive diffraction peaks of NIT persisted with a marked decrease in their intensity compared with the PMs of the same ratio, indicating a decrease in the crystallinity of NIT. At the ratio of 1 : 5 (Fig. 3 H), the diffraction pattern became hollow, indicating an amorphous state of NIT and the form of SD.

DSC Curves DSC curves and a fusion enthalpy-melting point graph of the NIT–HPMCP system are shown in Fig. 4 and Fig. 6a, respectively. A DSC thermogram of pure NIT showed a sharp endothermic peak with an onset melting temperature of 158 °C and a fusion enthalpy (ΔH) of about 94.66 J/g, whereas HPMCP exhibited a broad endothermic peak, owing to its amorphous nature. The PMs showed endothermic peaks corresponding to pure NIT. Furthermore, as evident from Fig. 6a, the crystallization peaks of PMs shifted toward a lower temperature and the ΔH of the endothermic peaks decreased as the ratios of HPMCP increased. These indicated the interaction between NIT and HPMCP in PMs. SDs at a ratio of 1 : 1 and 1 : 3 (Fig. 4 F, G) prepared by the twin screw extruder method showed a NIT-derived endothermic peak with lower melting temperature and ΔHs of 20.45 J/g and 1.69 J/g respectively (Fig. 6a E, F), suggesting the existence of small quantities of NIT crystals, while 1 : 5 NIT–HPMCP SD (Fig. 4 G) showed a broad curve with no endothermic peak corresponding to the melting of pure crystalline NIT. This observation confirmed that NIT changed to an amorphous state in mixtures of NIT–HPMCP and the SDs were formed when treated with the twin screw extruder method.

DSC thermograms and a fusion enthalpy-melting point graph of the NIT–CAR system are presented in Fig. 5 and Fig. 6b, respectively. Both PMs and SDs exhibited melting peaks of NIT (Fig. 5). There was no appreciable shift in the melting point of NIT in the PMs with CAR (Fig. 6b B—D). However, the DSC thermogram for the SDs of NIT and CAR indicates an obvious decrease in the melting point of NIT (Fig. 6b E—G). This signifies some form of interaction between NIT and CAR that is more prominent in an SD than in a PM. In addition, an appreciable decrease in ΔH (Fig. 6b E—G) was observed, indicating the formation of an SD.

NIT crystals were not detected in the 1 : 5 NIT–CAR SD with powder X-ray diffraction analysis, but the DSC measurement revealed an endothermic peak and the enthalpy change of the mixtures was about 11.3% of NIT crystals, suggesting the existence of a small quantity of NIT crystals in mixtures.

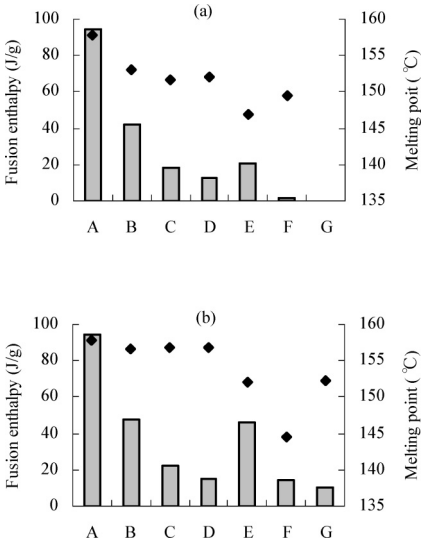

Fig. 6. Fusion Enthalpy and Onset Melting Temperature of NIT–HPMCP and NIT–CAR Systems

(a), NIT–HPMCP system; (b), NIT–CAR system; A, NIT; PMs, NIT : carrier, B, 1 : 1; C, 1 : 3; D, 1 : 5; twin screw extruder method, NIT : carrier, E, 1 : 1; F, 1 : 3; G, 1 : 5. ▩, fusion enthalpy; ◆, onset melting temperature.

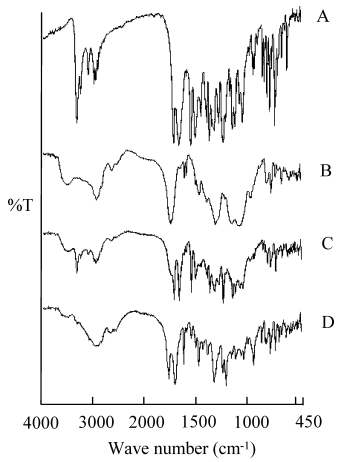

Fig. 7. IR Spectra of NIT and NIT–HPMCP PMs and SDs

A, NIT; B, HPMCP; C, PM (NIT : HPMCP = 1 : 3); D, twin screw extruder method (NIT : HPMCP = 1 : 3).

These findings revealed that the twin screw extruder method were found to have made NIT amorphous in NIT–HPMCP and NIT–CAR systems and formed SDs.

Confirmation of Interactions Using IR Spectrometry In order to test for possible intermolecular interactions between nitrendipine and the constituents of the dispersion matrix, FT-IR was used. FT-IR spectra obtained with samples prepared using the twin screw extruder method with HPMCP as the carrier are shown in Fig. 7, and those obtained with samples containing CAR as the carrier are shown in Fig. 8. NIT alone and the PM of NIT–HPMCP (1 : 3) showed N–H stretching vibrations at 3316.6 and 3317.4 cm^{-1}, respectively, due to the secondary amine groups (–NH–) of NIT (Fig. 7 A, C) and for HPMCP a peak characteristic of the O–H stretching vibration of the hydroxyl groups was observed at 3498 cm^{-1} (Fig. 7 B), while in the 1 : 3 (NIT : HPMCP) SD prepared with the twin screw extruder method, the N–H and O–H stretching vibrations disappeared (Fig. 7 D). This finding suggested that the formation of solid dispersions of NIT and HPMCP using the twin screw extruder method was due to interactions of the two components, and that hydrogen bonding between the secondary amine groups of NIT and hydroxyl group groups of HPMCP is involved in these interactions.

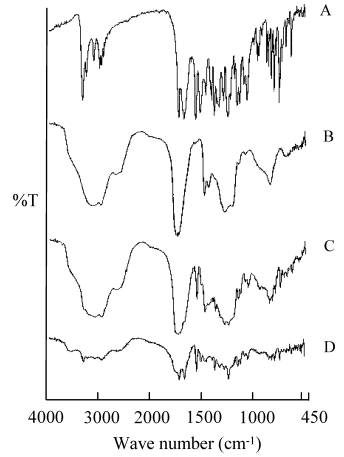

Fig. 8. IR Spectra of NIT and NIT–CAR PMs and SDs

A, NIT; B, CAR; C, PM (NIT : CAR = 1 : 3); D, twin screw extruder method (NIT : CAR = 1 : 3).

From Fig. 8, the characteristic secondary amide group (N–H) stretching vibration at 3316.6 cm^{-1} for NIT alone was not observed in the IR spectrum of 1 : 3 (NIT : CAR) PM (Fig. 8 C) and appeared to be conspicuously less sharp and shifted to 3317.6 cm^{-1} in 1 : 3 (NIT : CAR) SD (Fig. 8 D) prepared with the twin screw extruder method. The characteristic absorption peak at 3115 cm^{-1}, due to the hydroxyl groups for CAR (Fig. 8 B), shifted to 3090 cm^{-1} in the IR spectrum of the PM and disappeared in the SD, and a band around 1715 cm^{-1} representing the stretching vibration of the carboxyl groups of CAR (Fig. 8 B, C) in the PM appeared to be significantly less sharp and shifted to 1700 cm^{-1} in the 1 : 3 (NIT : CAR) SD. The difference in the IR spectrum was attributed to the hydrogen bonding between the secondary amine groups of NIT and carboxyl groups of CAR during formation of the solid dispersion.

Additionally, the IR spectrum of NIT : CAR (1 : 3) SD showed an N–H stretching vibration which was not observed in the NIT : HPMCP (1 : 3) SD, indicating stronger interactions between NIT and HPMCP than between NIT and CAR.

Dissolution Test Dissolution profiles of NIT from NIT–HPMCP systems in 0.5% SDS (w/v) are shown in Fig. 9 and the relationship between the apparent dissolution rate constant (K_p) and the ratios of HPMCP in the samples are illustrated in Fig. 11A. Figure 9A compared the mean% NIT dissolved from PMs containing different proportions of HPMCP in 0.5% SDS (w/v) *versus* time. The dissolution of the 1 : 3 NIT–HPMCP PM was merely higher than those of others. However, as shown in Fig. 11A, no significant difference was observed between the K_p of pure NIT and the PMs. Figure 9B is a comparative plot of the dissolution profiles in 0.5% (w/v) SDS for NIT from SDs prepared with the twin screw extruder method. According to the results from powder X-ray diffraction and DSC analysis, the 1 : 3 and 1 : 5 NIT–HPMCP SD were thought to have formed SDs. How-

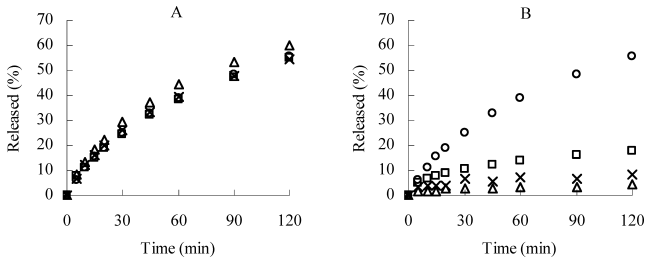

Fig. 9. Dissolution Profiles of NIT from NIT–HPMCP Systems

A, PMs; B, twin screw extruder method. ○, NIT; □, 1 : 1; △, 1 : 3; ×, 1 : 5. Each point represents the mean (n=3).

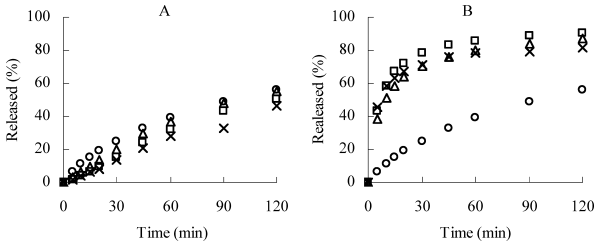

Fig. 10. Dissolution Profiles of NIT from NIT–CAR Systems

A, PMs; B, twin screw extruder method. ○, NIT; □, 1 : 1; △, 1 : 3; ×, 1 : 5. Each point represents the mean (n=3).

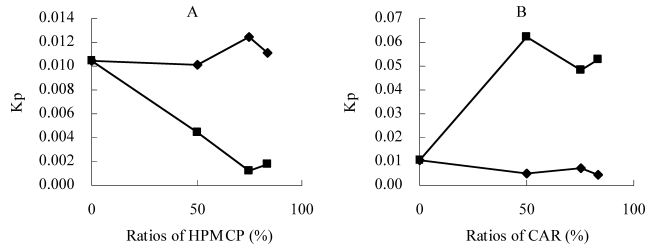

Fig. 11. Relationship between K_p of NIT from NIT–HPMCP and NIT–CAR Systems and Ratios of Carriers

A, NIT–HPMCP system; B, NIT–CAR system. ◆, PMs; ■, twin screw extruder method.

ever, to the contrary, a significant decrease in the dissolution of NIT was observed in the case of the SDs compared with pure NIT and PMs. This could be ascribed to the difficulty in breaking the tight interaction due to the hydrogen bonding between NIT and HPMCP formed during the preparation using the twin screw extruder method. Dissolution of NIT from 1 : 1 NIT–HPMCP SD was slightly higher than from 1 : 3 and 1 : 5 NIT–HPMCP SD (Fig. 11A). This may be due to the interaction between NIT and HPMCP being more prominent in 1 : 3 and 1 : 5 SD than in 1 : 1 SD, which led to a decrease in the dissolution of 1 : 3 and 1 : 5 SD.

Dissolution profiles of NIT from NIT–CAR systems and the relationship between K_p and the ratios of CAR in samples are shown in Fig. 10 and Fig. 11B, respectively. A decrease in the dissolution of NIT was observed in the case of NIT–CAR PMs (Fig. 10A) with increasing ratios of CAR. K_p for PMs also decreased from 0.0104 to 0.0045 min^{-1} (Fig. 11B). This was due to the absence of interaction between NIT–CAR PMs and the formation of a thick hydrogel layer of CAR immediately after the addition of PMs to 0.5% SDS (w/v), leading to the adherence of granules to each other to slow the dissolution of NIT from PMs. Figure 10B showed the dissolution profiles of NIT from SDs in 0.5% SDS (w/v). Dissolution of NIT from all SDs was significantly higher than from pure NIT and PMs. K_p for SDs was markedly improved from 0.0104 to 0.0622 min^{-1} (Fig. 11B). This could be attributed to the ready dispersion of NIT into the fishnet structure of CAR when treated with the twin screw extruder and the rapid release as a result of the channel generated by the swelling of CAR.

Conclusions

(1) Powder X-ray diffraction and DSC evaluation indicated that when NIT–HPMCP and NIT–CAR mixtures were treated using a twin screw extruder method, the crystallinity of NIT decreased and it changed to an amorphous state in the mixtures and that solid dispersions can be formed by the process of heating/pressurization/kneading/extruding.

(2) As shown in the IR spectra obtained with the 1 : 3 (NIT : HPMCP) SD prepared by the twin screw extruder method, the disappearance of the N–H stretching vibration due to the secondary amine groups (–NH–) of NIT and O–H stretching vibration due to the hydroxyl groups of HPMCP, which were observed for the PM and HPMCP respectively, indicated the presence of hydrogen bonding between NIT and HPMCP. In the case of NIT–CAR (1 : 3) SD, the decrease and shift of the N–H stretching vibration, the absence of the O–H stretching vibration, which were observed for the PM and CAR, respectively, and the shift of the stretching vibration of the carboxyl groups of CAR also proved the interaction of hydrogen bonding between the secondary amine groups of NIT and the carboxyl groups of CAR during the formation of the solid dispersion.

(3) No significant difference was observed between the dissolution of pure NIT and PMs containing different ratios of HPMCP as a carrier. However, the dissolution of NIT–HPMCP SDs prepared with the twin screw extruder method markedly decreased compared with pure NIT and PMs. In the evaluation of the NIT–CAR system, SDs containing different proportions of CAR were found to give significantly higher dissolutions than pure NIT and PMs, while no increase in dissolution rate was observed when the ratios of CAR in the SDs increased.

These findings indicated that when the twin screw extruder was employed to prepare SDs, CAR, used as a carrier, has a greater ability to improve the dissolution of NIT than does HPMCP. This can also be explained by the intermolecular interactions between NIT and HPMCP, which was proven by the FT-IR spectra to be too strong for the drug to be released from the carriers.

(4) The twin screw extruder method can be used as a simple and effective method for the preparation of solid dispersions to improve the dissolution properties of poorly water-soluble drugs when choosing proper polymers as carriers.

Acknowledgements We are grateful to Professor Isamu Maeba of Meijo University and Li Yan, Shenyang Pharmaceutical University, for their help in the determination of FT-IR spectra. The author also wishes to express thanks to Yorinobu Yonezawa and Shinichiro Yasui, for their help during the experiment.

References

1) Sekiguchi K., Obi N., *Chem. Pharm. Bull.*, **9**, 866—872 (1961).
2) Chiou W. L., Riegelman S., *J. Pharm. Sci.*, **59**, 937—942 (1970).

3) Chiou W. L., Riegelman S., *J. Pharm. Sci.*, **60**, 1281—1302 (1971).
4) Sugimoto I., *Inphachem.*, **2**, 17—26 (1981).
5) Ford J. L., Stewart A. F., Rubinstein M. K., *J. Pharm. Pharmacol.*, **31**, 726—729 (1979).
6) Hasegawa A., Sugimoto I., *Kagaku Kogyo*, **37**, 309—317 (1986).
7) Summers M. P., Enever R. P., *J. Pharm. Sci.*, **65**, 1613—1617 (1976).
8) McGinity J. W., Zhang F., Repka M. A., Koleng J. J., Matsuda Y., *Pharm. Tech. Jpn.*, **16**, 897—913 (2000).
9) Hayakawa I., "Extrusion Cooking," KORIN, Tokyo, 1987, pp. 11—43.
10) Sakai T., *High Polymers Jpn.*, **42**, 768—771 (1993).
11) Nakamichi K., Yasuura H., Fukui H., Oka M., Izumi S., Andou T., Shimizu N., Ushimaru K., *Yakuzaigaku*, **56**, 15—22 (1996).
12) Verreck G., Six K., Van den Mooter G., Baert L., Peeters J., Brewster M., *Int. J. Pharmaceut.*, **251**, 165—174 (2003).
13) Rambali B., Verreck G., Baert L., Massart D. L., *Drug Dev. Ind. Pharm.*, **29**, 641—652 (2003).
14) Six K., Verreck G., Peeters J., Brewster M., Van Den Mooter G., *J. Pharm. Sci.*, **93**, 124—131 (2004).
15) Kinoshita M., Baba K., Nagayasu A., Yamabe K., Shimooka T., Take-ichi Y., Azuma M., Houchi H., Minakuchi K., *J. Pharm. Sci.*, **91**, 362—370 (2002).
16) Mikus G., Eichelbaum M., *J. Cardiovasc. Pharmacol.*, **9**, S140—S141 (1987).
17) Hasegawa G. R., *Clin. Pharm.*, **7**, 97—108 (1988).
18) Zhu Z. Y., Mao F. F., Zhu J. B., *Yao Xue Xue Bao*, **25**, 709—716 (1990).